Article

Probing and Controlling Dynamic Interactions at Biomolecule –Nanoparticle Interfaces Using Stochastic DNA Walkers

Sean D Mason, Guan A Wang, Peng Yang, Yongya Li, and Feng Li

ACS Nano, **Just Accepted Manuscript** • DOI: 10.1021/acsnano.9b03053 • Publication Date (Web): 24 Jun 2019

Probing and Controlling Dynamic Interactions at Biomolecule-Nanoparticle Interfaces Using Stochastic DNA Walkers

Sean D. Mason,[†] Guan A. Wang,[†] Peng Yang,[†,‡] Yongya Li,[†] Feng Li[†,‡,]*

[†]Department of Chemistry, Centre for Biotechnology, Brock University, 1812 Sir Isaac Brock Way, St. Catharines, Ontario, Canada, L2S 3A1

[‡]College of Chemistry, Analytical & Testing Centre, Sichuan University, Chengdu, China, 610064

*Corresponding Author: fli@brocku.ca

Abstract

Herein, we report a bottom-up approach to assemble a series of stochastic DNA walkers capable of probing dynamic interactions occurring at the bio-nano interface. We systematically investigated impact of varying interfacial factors, including intramolecular interactions, orientation, cooperativity, steric effect, multivalence, and binding hindrance on enzymatic behaviors at the interfaces of spherical nucleic acids. Our mechanistic study has revealed critical roles of various interfacial factors that significantly alter molecular binding and enzymatic behaviors from bulk solutions. The improved understanding of bio-nano interface may facilitate the better design and operation of nanoparticle-based biosensors and/or functional devices. We successfully demonstrate

how improved understanding of bio-nano interface help rationalize the design of amplifiable biosensors for nucleic acids and antibodies.

keywords

bio-nano interface, DNA walker, biosensor, enzyme activity, antibody detection

Biohybrid inorganic nanoparticles (NPs) have offered exciting opportunities in material, biological and medical sciences with applications ranging from biosensing,[1-3] to gene regulation,[4] to drug delivery,[5] and to the fabrication of diverse structures and devices.[6-8]

While much effort has been emphasized on the synthesis, functionality, and applications of NPs, it is also critical to understand and control dynamic interactions at the biomolecular-nanoparticle (bio-nano) interfaces. This is because molecular interactions, such as affinity bindings and enzymatic catalysis at bio-nano interfaces are often influenced by multiple interfacial factors, such as valence, binding hindrance, adsorption, orientation, and curvature effects, and thus may differ significantly from those in bulk solutions.[9-11] It has been well documented that multivalent, ligand-modified NPs are often of enhanced binding affinities compared to isolated ligands.[12] A growing number of recent studies also suggest that polyvalent, substrate-modified NPs can accelerate enzymatic reactions compared to freely diffused substrate in bulk solution.[13,14] On the other hand, Seferos *et al.* found that DNA substrates functionalized to gold NPs (AuNPs) presented a strong resistance to degradation by deoxyribonuclease I.[15] In a following study, Pridogich *et al.* further demonstrated that it was possible to regulate enzyme activities using the DNA-AuNP interface which selectively enhanced ribonuclease H while inhibiting other nucleases.[16] Given the critical role of bio-nano interfaces in mediating molecular interactions, we reasoned that

strategies capable of fine-tuning and probing the interfacial environment might lead to better understanding and thus offer opportunities for rationalizing the design and uses of NPs. Herein, we report a bottom-up approach to rationally design and assemble a series of enzymatic systems with tunable interfacial microenvironments and thus allow the interrogation of the specific roles of varying factors at the bio-nano interface.

Our idea is inspired by the recent advances of stochastic DNA walkers capable of traversing on three dimensional (3D) tracks made of spherical nucleic acids (SNA).[17-21] We hypothesize that enzyme-powered stochastic 3D DNA walkers are ideal system to probe and control dynamic interactions at bio-nano interfaces. Contrary to existing enzyme-NP systems where intraparticle movement of enzymes are dominated by nonspecific adsorptions,[9,10] the persistent movement of DNA walkers and subsequent enzymatic reactions are mediated by the exquisite Watson-Crick base-pairing and thus are highly predictable and programmable. As such, we design a SNA track and a series of DNA walkers and demonstrate the critical roles of varying interfacial factors, including intraparticle interaction, orientation, cooperativity, steric effect, multivalence, and binding

hindrance. Using the improved understanding of enzymatic behaviors at the SNA interface, we also successfully develop two biosensors for amplified detection of nucleic acids and proteins.

Results and Discussion

Design Principle. Molecular interactions at the bio-nano interface may differ significantly from that of a bulk solution. For example, enzymatic activities in a bulk solution are dominated by molecular colliding (Scheme 1A), the kinetics of which can be quantitatively described using the classic Michaelis-Menten (MM) model (Eq 1), where V is the rate at a substrate concentration [S], K_M is the Michaelis constant, V_{max} is the maximum rate which is determined by the catalytic rate constant k_{cat} and enzyme concentration $[E]_0$ (e.q. 2).

$$V = V_{max}\frac{[S]}{K_M + [S]} \qquad (1)$$

$$V_{max} = k_{cat}[E]_0 \qquad (2)$$

However, enzymatic activities can be far more complicated at the bio-nano interface, involving intraparticle interactions resulting from non-specific adsorption and varying interfacial factors (Scheme 1B).[9-14] An ideal substrate-NP system for probing enzymatic activities shall allow the independent control and interrogation of each factor. As such, we designed a series of nicking endonuclease powered stochastic 3D DNA walkers with SNA track as the bio (DNA)-nano (AuNP) interface. Each enzyme-powered walking step involves the following three elementary reactions:

$$\textbf{Reaction 1: } S + W \underset{k_{-1}}{\overset{k_1}{\rightleftharpoons}} SW$$

$$\textbf{Reaction2: } SW + E \underset{k_{-2}}{\overset{k_2}{\rightleftharpoons}} SWE$$

$$\textbf{Reaction 3: } SWE \xrightarrow{k_{cat}} W + E + P$$

where W represents the DNA walker, S represents the substrate, P is the product, and E is the nicking endonuclease. When supplying excess amount of nicking endonucleases, intermediates SW and SWE will be consumed rapidly. The quasi-steady-state assumption can thus be applied, where

$$\frac{d[SW]}{dt} = k_1[S][W] + k_{-2}[SWE] - k_{-1}[SW] - k_2[SW][E] = 0 \qquad (3)$$

$$\frac{d[SWE]}{dt} = k_2[SW][E] - k_{-2}[SWE] - k_{cat}[SWE] = 0 \qquad (4)$$

The rate of the overall reaction V can then be derived as:

$$V = \frac{d[P]}{dt} = \frac{\frac{k_1 k_2[E] k_{cat}[W]_0}{k_1 k_2[E] + k_1 k_{-2} + k_1 k_{cat}} \cdot [S]}{\frac{k_{-1} k_{-2} + k_{-1} k_{cat} + k_2[E] k_{cat}}{k_1 k_2[E] + k_1 k_{-2} + k_1 k_{cat}} + [S]} \qquad (5)$$

As nicking endonuclease is in large excess, [E] can be replaced with [E]0 and the equation can be further simplified as:

$$V = \frac{{V_m}^* \cdot [S]}{{K_m}^* + [S]} \qquad (6)$$

$${V_m}^* = \frac{k_1 k_2[E]_0 k_{cat}[W]_0}{k_1 k_2[E]_0 + k_1 k_{-2} + k_1 k_{cat}} = k_{cat}^*[W]_0 \qquad (7)$$

$${K_m}^* = \frac{k_{-1} k_{-2} + k_{-1} k_{cat} + k_2[E]_0 k_{cat}}{k_1 k_2[E]_0 + k_1 k_{-2} + k_1 k_{cat}} \qquad (8)$$

The mathematic derivatization suggests that the behavior of a DNA walker (*W*) follows the MM model and is effectively an enzyme in our system.

The design of a specific bipedal DNA walker (BDW) is illustrated in Scheme 1C. The SNA track is created by conjugating hundreds of fluorescently labeled single-stranded DNA (ssDNA) substrate to a 20 nm AuNP through the well-established gold-thiol chemistry.[22,23] Each substrate contains a 7-nt nicking cleavage sequence. BDW is a ssDNA containing the 7-nt nicking recognition sequence (the foot) at both 5' and 3' ends. Because of the base complementarity, BDW can bind to the SNA track at the DNA-AuNP interface. In the presence of nicking endonuclease, BDW cleaves the substrate and walks along the interface (intraparticle interaction). When both feet cleave substrates at the same time, BDW dissociates and diffuses back into the bulk solution. As each walking step releases a fluorophore labeled cleavage product, the dynamic interactions between BDW and track can be monitored in real-time. Varying interfacial factors can be controlled and probed by introducing variants in the walker or tuning the SNA track.

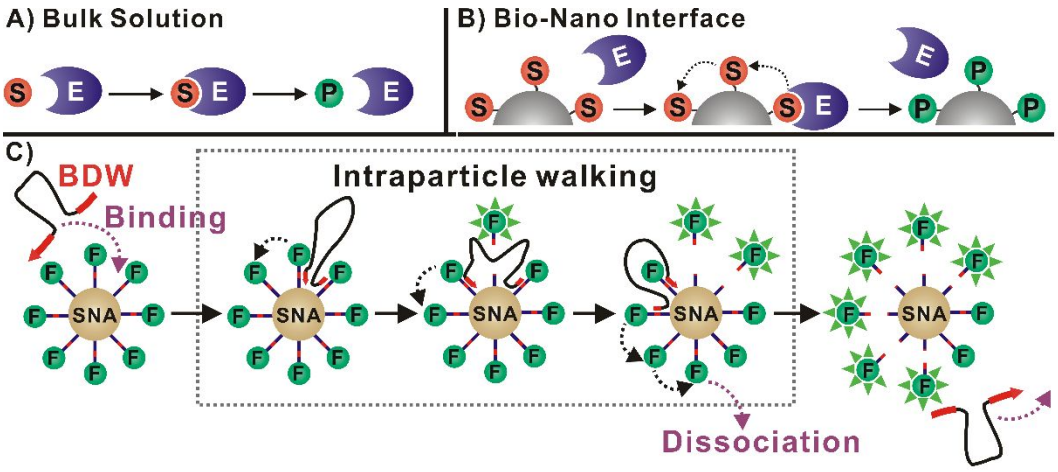

Scheme 1. Schematic illustration of enzyme-substrate interaction in bulk solution (**A**) and at the bio-nano interface (**B**). (**C**) An enzyme-powered bipedal DNA walker (BDW) capable of traversing at the bio-nano interface created by a spherical nucleic acid (SNA) track. The red domains of BDW represent nicking recognition sequences and those of SNA substrates represent nicking cleavage sequences. The nicking endonuclease is omitted from the figure for better visual presentation.

Intraparticle Interactions. Intraparticle interaction is one of the most important interfacial factors that complicate the enzymatic behavior at the bio-nano interface. Depending on the reversibility of the intraparticle interaction, an enzymatic reaction at bio-nano interface can be modeled as a hopping mechanism (reversible intraparticle interaction)

or a scooting mechanism (irreversible intraparticle interaction).[14] However, intraparticle interactions in most enzymatic systems are driven by the nonspecific adsorption which is difficult to control and measure. Therefore, the exact role of intraparticle interaction and the enzymatic behavior at the bio-nano interface could only be deduced through indirect measurements and mathematical fitting.[9]

Towards this challenge, we first set to engineer two DNA walker systems that provide programmable intraparticle interactions through DNA hybridization. The BDW was designed to have two 8-nt feet at both 3' and 5' ends (Figure 1A). As a result, BDW can bind stably with the SNA track in the absence of the nicking endonuclease. Although both feet contain the nicking recognition sequence, we found that the catalytic efficiency of the 3' foot was much higher than that of the 5' foot. This difference allows for several intraparticle walking steps before a complete dissociation and hopping to another SNA track, which mimics reversible adsorption commonly seen in many enzyme-NP systems.[9,10] To quantitatively probe the role of intraparticle interaction, we designed two SNA tracks that were of the same substrate sequence and density (~150 per SNA), but

labeled with fluorescent amidite (FAM, F-Track) and tetramethyl rhodamine (TAMRA, T-Track), respectively (Figure 1A). BDW was first primed on the F-Track and then mixed with the T-Track for 10 min before adding the nicking endonuclease. By monitoring fluorescence signals generated by both tracks in real-time, we found that BDW reacted predominately on the F-track in the first 6 min with an average rate of 2 substrates per NP per minute. The signal at T-track was then increased drastically beginning at 7 min. Correspondingly, a near 4-fold drop of the cleavage rate was also observed at the F-Track, suggesting that the reversible intraparticle interaction has led to a hopping mechanism and each BDW could take averagely 12 persistent steps at the SNA interface before hopping to another NP. We also noticed that BDW consistently prefers T-Track over F-Track (Figure 1B and S1) under the same substrate sequence and density, suggesting that subtle chemical changes (TAMRA over FAM) at the interface may also alter the enzymatic behavior.

To assemble an enzyme-NP system with irreversible intraparticle interaction, we next modified BDW by replacing the 5' nicking recognition sequence with a 12-nt poly-

adenine (poly-A) foot that hybridizes to the poly-thymine (poly-T) spacer of the substrate (Figure 1C). Therefore, the DNA walker (referred as TDW) can be tethered on the SNA track through the 5' poly-A foot while the 3' foot remains enzymatically active. Once primed on the F-track and interrogated using the T-Track (Figure 1C), we found that TDW cleaved predominately at the F-Track (Figure 1D), suggesting that scooting mechanism could be realized through an irreversible intraparticle interaction.

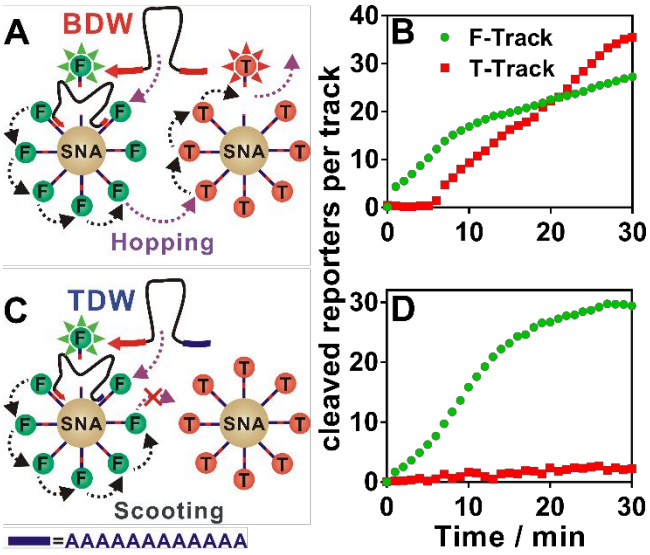

Figure 1. Probing and controlling intraparticle interaction using bipedal DNA walkers. (**A**) Probing reversible intraparticle interactions commonly involved in enzymatic reactions at bio-nano interface using a BDW and two fluorescently labeled SNA tracks. (**B**) Kinetic profile of BDW that is initially primed on F-Track and then mixed with T-Track. To

compare fluorescent signals at two different channels, fluorescence readout was first converted into the total concentration of released reporters ($[reporter]_{released}$). The **cleaved reporters per track** = $[reporter]_{released}$/[F-Track] (or [T-Track]). [BDW] = 250 pM, [F-Track] = [T-Track] = 500 pM, [nicking endonuclease] = 10 unit. (**C**) Probing the role of irreversible intraparticle interactions on the kinetics of enzymatic reactions at the bio-nano interface using a tethered DNA walker (TDW). (**D**) Kinetic profile of TDW that is initially primed on F-Track. [TDW] = 250 pM, [F-Track] = [T-Track] = 500 pM, [nicking endonuclease] = 10 unit.

Orientation, Cooperativity, and Steric Hindrance. When densely functionalized on a NP, substrates may behave significantly different from those in a homogenous solution. Such heterogeneity also complicates the biorecognition and enzymatic activities at bio-nano interfaces. The steric hindrance and nearest-neighbor interactions often hinder mutually favorable orientations between enzyme and substrate.[10] The multivalence, on the other hand, may promote enzymatic activities through enhanced binding affinity and cooperativity.[12-14] To probe and control each interfacial factor, we modified BDW into a

series of DNA walkers that are sensitive to orientation, cooperativity, or steric hindrance (Figure 2).

We first probed the effect of orientation by modifying BDW into two single-foot DNA walkers that only contain the 3'-foot (3'SDW) or the 5'-foot (5'SDW). When compared to BDW, 3'SDW and 5'SDW became much less efficient for cleaving substrates from the SNA track (Figure 2A). This is to be expected as there is no second foot to allow the intraparticle walking. More importantly, though the spacer sequences are identical for both single feet, the 3'SDW maintained a near 25% activity while 5'SDW was nearly completely deactivated, suggesting that the orientation of the walker played a critical role at the interface. More specifically, to maintain the anti-parallel base-pairing with substrates, the 5'SDW needs to fold its orientation to expose the nicking recognition sequence, whereas the 3'SDW can insert readily into the layer of substrate (Figure S2). Despite the unfavored orientation, we also found that the 5' foot of BDW may still bind and cleave the substrate, evidenced by the observation that BDW with a deactivated 3'-foot (M-BDW) could still maintain nearly 10% activity (Figure 2A). To further understand

the role of orientation for BDW, we selectivity deactivated 3' foot or 5' foot by introducing a protecting DNA that partially blocks the nicking recognition sequence through hybridization (Figure 2B). We have previously shown that this strategy could completely deactivate a DNA walker that was co-conjugated with substrates on the same AuNP.[19] When placing the protection at 5'-foot, BDW was partially deactivated, with an activity (~30% of the unprotected walker) slightly higher than that of the 3'SDW (~25%). Surprisingly, when placing the protection at 3' end, the activity of BDW was still 30%, which was significantly higher than that of the 5'SDW. This observation is consistent with our speculation that 5' foot could still initiate binding with SNA, which leads the protected 3' foot in close proximity to the substrate. As a result, the activity of 3' foot could be partially restored through a strand exchange between substrate and the protecting strand. A near complete deactivation could only be achieved when both feet were deactivated through hybridization (Figure 2B), suggesting that strong cooperativity existed between the two feet. We also found that the cooperative behavior of the two feet was distance and rigidity dependent. An optimal spacer length existed, which maximized the kinetics of cleavage (Figure S3). By replacing the flexible ssDNA spacer

of BDW with a more rigid duplex spacer, we observed a reduction of activity by 30% (Figure S4).

We finally probed the steric effect by chemically modifying BDW with a biotin molecular at the 3' end (Figure 2C). This chemical modification slightly increases the bulkiness of BDW, which resulted in a decrease of activity by ~30%. The activity of BDW was completely deactivated when a large bulky streptavidin was introduced to the 3' end through the strong streptavidin-biotin interaction, suggesting the steric hindrance may become significant when bulky groups exist at the bio-nano interface.

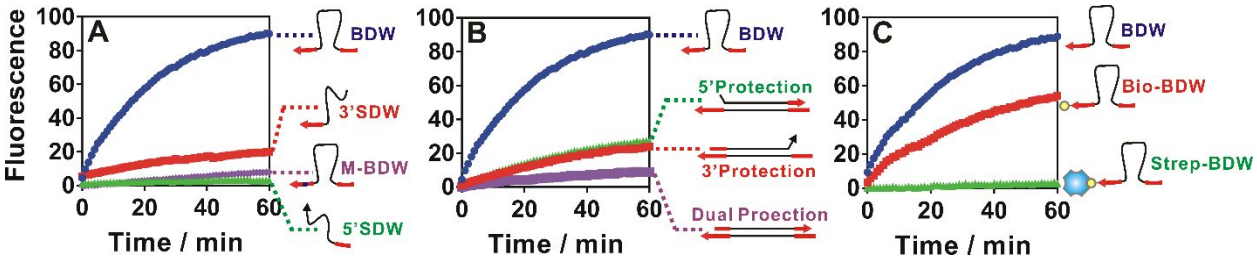

Figure 2. Quantitatively determining the effect of orientation (**A**), cooperativity (**B**) and steric hindrance (**C**) on enzymatic activities at the bio-nano interface using varying DNA walker designs. In all experiments, [Walker] = 500 pM, [F-Track] = 500 pM, [nicking

endonuclease] = 10 unit. The substrate density on each F-Track was estimated to be ~400 on average. The concentration of streptavidin was 1 nM.

By probing the effect of each interfacial factor, we were able to better understand the DNA walking behavior at the SNA interface. The proposed mechanisms for the four representative DNA walkers are outlined in Scheme 2. BDW is the most efficient DNA walker because of the favored orientation at 3' end, the high binding cooperativity, and intraparticle interactions (Scheme 2A). Although there was only one foot, the 3'SDW maintains a ~25% activity because of the favored orientation (Scheme 2B). For a 5'SDW, the 5' foot may still bind to the SNA track, but because of the unfavored orientation and charge repulsion, it dissociated rapidly before triggering enzymatic cleavage (Scheme 2C). The streptavidin-modified BDW, on the other hand, completely blocks the binding and enzymatic reactions, leading to a complete deactivation of BDW (Scheme 2D).

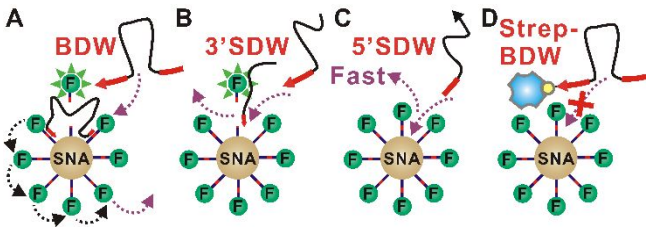

Scheme 2. Proposed mechanisms of BDW (**A**), 3'SDW (**B**), 5'SDW (**C**), and streptavidin-modified BDW (**D**) for binding and interacting with SNA track based on the experimental observation in Figure 2.

Multivalence *vs.* Binding Hindrance. Having investigated varying interfacial factors by designing a series of DNA walkers, we then explored the impact of interfacial environment on intraparticle interactions and the initial binding between BDW and SNA track. Interfacial environment, such as the density of substrate, on each SNA has a direct impact on important interfacial factors such as multivalence and binding hindrance (steric hindrance and charge repulsion). Therefore, we aim to control interfacial environment by fine-tuning the substrate density at the SNA interface.

We first explored the impact of substrate density on the intraparticle interaction. To exclude the influence of the initial binding step, BDW was primed on SNA before

subjecting to enzymatic cleavage. By monitoring the fluorescence increase in real-time, we found that the initial rate V of the enzymatic reaction was independent from the density or the concentration of SNA (Figure S5), suggesting that the intraparticle interaction was dominated by the local effective concentrations of substrates rather than the multivalence or binding hindrance. The effective concentration ([S]) remains much higher than K_M^* (eq. 6) because of the ultrasmall volume the reactants occupying (< 30 zL) and high effective concentration (> 200 μM). Therefore, V equals to the maximal initial rate V_{max} throughout varying experimental conditions (eq. 7). We also found that V is linearly related to the concentration of BDW (Figure S5C), suggesting that the apparent catalytic rate constant k_{cat}^* is also independent of the interfacial environment.

We next evaluated the effect of substrate density on the binding between BDW and SNA, as both multivalence and binding hindrance may have a direct but opposite impact on the binding step. However, it is difficult to directly probe the binding step by monitoring the fluorescence, as it is coupled with the subsequent intraparticle walking. As such, we introduced a low-density T-Track (~150 substrates per SNA) as a reference

interface, which was mixed with either a high-density F-Track (HD-Track, ~400 substrates per SNA) or a low-density F-Track (LD-Track, ~150 substrates per SNA). Upon mixing with BDW, the two tracks (T-Track and F-Track) competed for binding with BDW (Figure 3A). We then measured the initial rates of both tracks using the fluorescence signals collected in both channels (Figure S6), the ratio ($V_{F\text{-}Track}/V_{T\text{-}Track}$) of which was plotted in Figure 3B. The ratio for the HD-Track was found to be 4-fold higher than that of the LD-Track, suggesting that multivalence dominates the binding step and interface of higher substrate density is more competitive for binding. We also found that binding hindrance is more significant for the 5'SDW that is sensitive to the binding orientation. Increases in enzymatic activities were observed at interface of lower substrate densities (Figure S7).

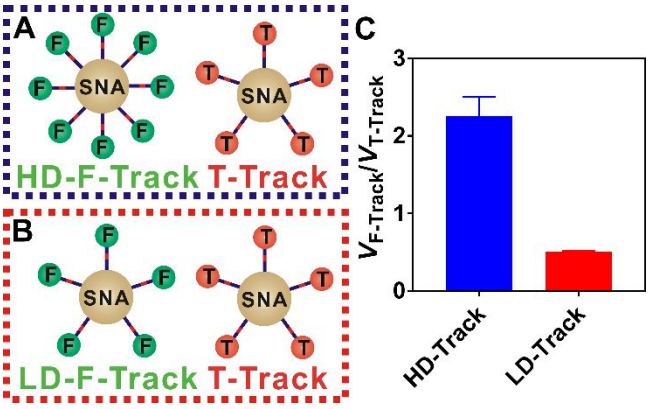

Figure 3. Effect of interfacial environment (multivalence *vs.* binding hindrance) on the initial binding between BDW and SNA track. BDW is interrogated using a mixture of high-density (HD) F-Track and a reference low-density (LD) T-Track (**A**) or a mixture of low-density (LD) F-Track and a reference LD T-Track (**B**). (**C**) Comparing the ratio of initial rates between F-Track and reference T-Track for HD-Track and LD-Track, respectively. [BDW] = 250 pM, [HD-F-Track] = [LD-F-Track] = [T-Track] = 500 pM, [nicking endonuclease] = 10 unit. Each error bar represents one standard deviation from triplicated analyses.

Rational Design of Biosensors. Our mechanistic study suggests that interfacial factors shall be considered when designing NP-based biosensors or functional devices. Here, we demonstrate that the conversion of our DNA walker systems to biosensors can be

rationalized by considering criteria drawn from the mechanistic study. First, DNA walkers with multiple binding and catalytic sites may drastically improve its activity through cooperative binding and intraparticle interactions. Second, the strong cooperativity of a bipedal DNA walker may require a protection strategy that deactivates both active sites. Third, the density of a SNA track shall be maximized to enhance the binding. Fourth, DNA walkers are sensitive to both orientation and steric hindrance. A biosensor may be designed by selectivity manipulate these properties in a target-specific manner. To realize the potential for translating the improved understanding of the bio-nano interface for biosensor development, we show two specific approaches for designing nucleic acid and protein sensors, respectively.

We first develop a nucleic acid sensor by sequestering a BDW using a protection sequence and then releasing BDW in a target nucleic acid (Figure 4 and Figure S8). As suggested in our mechanistic study, we maximized the density of SNA track to achieve favored binding. We also designed a protection sequence that blocked both 3'- and 5'-feet to achieve a complete deactivation of BDW. However, this protection probe

contains two sequence domains (4* and 6*) that are pre-defined by the nicking endonuclease. As such, the target sequence must be decoupled from the sequence of protection probe (*i.e.* the sequence of BDW). As such, we introduced an entropy-driven catalytic DNA circuit that selectively releases BDW in response to an input target (T).[25] As illustrated in Figure 4A, BDW is fully deactivated in a triplex substrate (S) containing a long ssDNA that complementary with BDW at domain 4*, 5* and 6*. S also contains a complementary sequence to T at domains 1*, 2* and 3* but with domains 2* and 3* protected by W1. T reacts with S through the toehold domain (1*) which releases W1 and expose another toehold (3*) on S. A fuel (F) strand then initiates strand displacement reaction with S through domain 3* and releases both BDW and T. BDW can then bind to the SNA track and T triggers another cycle of strand displacement. As a result, each target can release multiple BDW for subsequent enzymatic reactions. The dual signal amplification led to ultrasensitive detection of nucleic acid at a constant temperature (37 °C). A dynamic range of 100 fM to 100 pM (Figure 4B) and a detection limit of 10 fM were achieved. As the sequences of a target and BDW are completely

decoupled, our strategy is universal and generalizable to any target nucleic acid without the need for changing the design of BDW and SNA.

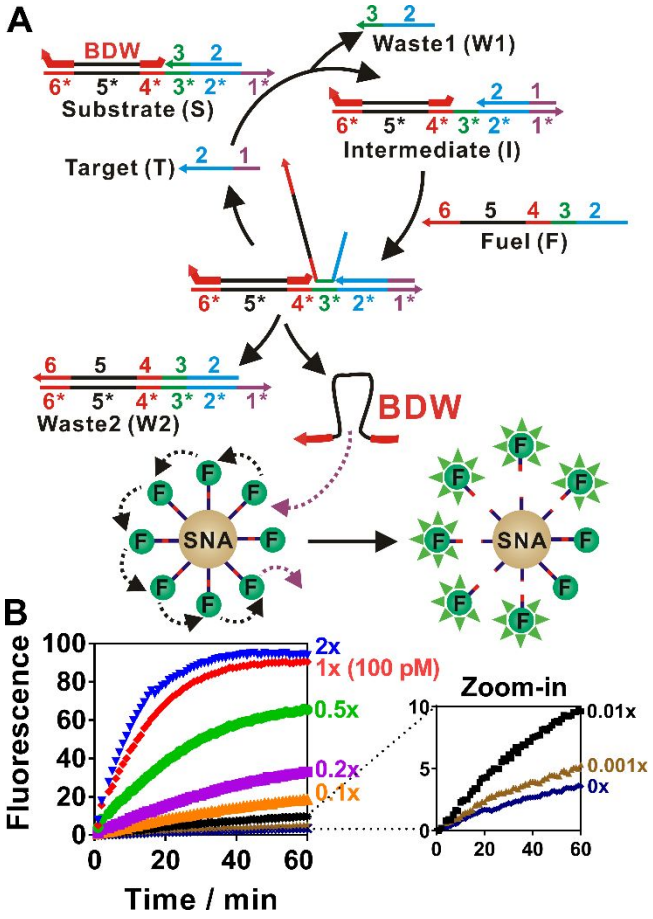

Figure 4. (**A**) Schematic illustration of target-specific activation of BDW using an entropy-driven catalytic DNA circuit. (**B**) Real-time monitoring the detection of target nucleic acid with concentrations varying from 100 fM to 200 pM. 1 × = 100 pM.

We finally engineered BDW system for the detection of antibodies (Figure 5 and Figure S9). Antibody-specific DNA nanodevices have shown exciting opportunities for point-of-care disease diagnosis.[25-28] Our mechanistic study has revealed the possibility for allowing the rapid, one-step, and amplified detection of antibodies or other proteins using stochastic DNA walkers. As BDW system is highly sensitive to steric hindrance at 3' end, the detection of antibodies can be achieved by modifying a small molecular antigen at 3' end of BDW (Figure 5A). As a proof-of-concept, we chose antibiotin antibody as a model input and modified BDW with biotin molecules. As shown in Figure 5C (red curve), the binding between the 3'-biotin and its antibody quantitatively deactivates the BDW, which generates a titration curve for antibody with concentrations ranging from 100 pM to 100 nM. We also modified BDW with biotin labels at both 3' and 5' ends, so that BDW became a bidentate binder with enhanced affinity to its antibody (Figure 5B). Indeed, a higher sensitivity was observed for this construct (Figure 5C, blue curve). Our success in designing and validating antibody-specific BDW suggests that a systematic mechanistic study of dynamic interaction at bio-nano interface may facilitate and accelerate the development of biosensors and nanodevices.

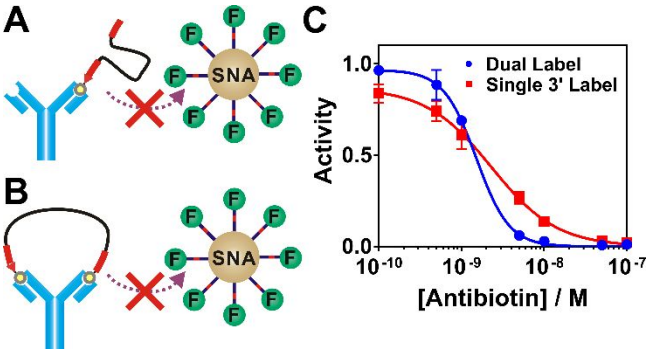

Figure 5. Schematic illustration antibody-specific BDWs by modifying 3' end with a biotin (**A**) or both 3' and 5' end with biotin molecules (**B**). (**C**) Titration curves of antibiotin antibodies using single-biotin modified BDW (red) or dual biotin modified BDW (blue). Each error bar represents one standard deviation from triplicate analyses.

Conclusion

To sum up, we have developed a bottom-up approach to assemble a series of stochastic DNA walkers capable of probing and controlling dynamic interactions at bio-nano interfaces on SNA. By monitoring dynamics of these DNA walkers on SNA tracks, we have systematically investigated the effect of important interfacial factors, including intraparticle interaction, orientation, cooperativity, steric effect, multivalence, and binding hindrance. Despite SNA is one of the most frequently used scaffolds to assemble various DNA nanosensors or nanodevices, impact of these interfacial factors has often been overlooked. Our mechanistic study has revealed critical roles of bio-nano interfaces, which shall be carefully evaluated for designing and operating NP-based biosensors or functional devices. As we have demonstrated theoretically and experimentally that the rate limiting step is the DNA hybridization rather than the enzymatic cleavage in our systems. We anticipate that conclusions of our mechanistic study can be generalized to other non-enzymatic DNA walker systems, such as those operated by catalytic DNA circuits.[29] We have also successfully adopted the improved understanding of bio-nano interface to rationalize the design of amplifiable biosensors for nucleic acids and proteins. Our success in systemic probing dynamic interaction at

bio-nano interfaces using DNA walkers also demonstrates the exciting opportunities that dynamic DNA nanotechnology can offer for addressing fundamental questions at the interface of chemistry and biology.

Methods

Chemicals and Materials. Solutions of gold nanoparicles (20 nm in diameter), magnesium chloride hexahydrate (MgCl2·6H2O), dithiothreitol (DTT), streptavidin from *Streptomyces avidinii*, and 10× phosphate-buffered saline (PBS) were purchased from Sigma Aldrich (Oakville, ON, Canada). Nb.BbvCI (10,000 units/mL) and 10x NEB CutSmart Buffer were purchased from New England BioLabs (Whitby, ON, Canada). Polyclonal anti-biotin antibody was purchased from Abcam. All DNA samples were purchased from Integrated DNA Technologies (Coralville, IA) and purified by high-performance liquid chromatography. The DNA sequences and modifications are listed in Table S1.

Preparation and Characterization of SNA Tracks. SNA tracks were prepared by conjugating fluorescently labeled ssDNA substrate onto AuNP according our previously

established method.[22] For a high-density track, substrate oligonucleotides were mixed with AuNPs at a ratio of 1000:1. This mixture was incubated at room temperature for 12 h and then was slowly mixed with 16.5 μL of 3 M NaCl, followed by 10 s of sonication. This process of addition of NaCl and sonication was repeated five times with a 1 h interval to maximize the oligonucleotide loading amounts.[23] The solution was then incubated at room temperature for 24 h. After incubation, the solution was centrifuged at 14 000 rpm for 30 min to separate the DNA-functionalized AuNPs (SNA) from the unreacted reagents. The SNA were washed three times with 1× PBS buffer (pH 7.4) containing 0.01% Tween 20 and finally re-dispersed in PBS buffer. After preparation, fluorescence spectroscopy was used to determine the coverage of substrate oligonucleotides on each AuNP.[30] Fluorescently labeled substrates were released from AuNP using 45 mM DTT. Fluorescence was measured using a multimode microplate reader (SpectraMax i3, Molecular Devices), and substrate coverage was quantified by using fluorescently labeled substrates as external standards. UV-Vis absorbance spectroscopy was used to determine the colloidal stability of newly prepared and stock SNAs (Figure S10). Long-term stability during 4 °C storage and short-term chemical

stability of SNA tracks were monitored using a fluorescence turn-on assay previously established by us.[22] The SNA tracks were found to be stable over 1-month storage at 4 °C (~2% reporter leakage at 25 days) and over 24-hr storage in NEB CutSmart Buffer at room temperature (~5% reporter leakage at 24 hrs). The activity of SNAs tracks that were stored short-termly in NEB CutSmart buffer or after long-time storage at 4 °C were also determined against BDW (Figure S11).

Real-Time Monitoring DNA Walkers on SNA Tracks. For a typical BDW reaction on SNA track, a reaction mixture containing DNA walkers of varying concentrations, SNA track of varying concentrations, and 1× NEB CutSmart buffer was added to a 96-well microplate. For experiments that require DNA walkers to be primed on the track, a pre-incubation of walker and designated track was carried out at 37° C for 30 min before adding the second track and nicking endonuclease. Fluorescence signals were measured immediately after adding the nicking endonuclease. This measurement was carried out at 37 °C measuring signal increase every 1 min using a multimode microplate reader with excitation/emission wavelength of 485/535 nm to monitor the

cleavage of FAM-labeled substrate and 550/580 nm for TAMRA-labeled substrate, respectively. The fluorescence signals were normalized by using a positive control containing 500 pM BDW and the SNA track (the saturated signal was set to be 100) and a negative control containing only the track (Figure S12). For mechanistic studies, the concentrations of DNA walkers were kept to be lower than those of the SNA tracks, so that each track accommodates no more than one walker on average.

Detection of Nucleic Acids. The DNA triplex (BDW/S/W) for entropy-driven catalytic circuit was prepared by mixing BDW, scaffold DNA (S), and a protecting DNA (W) at a ratio of 1:2:4. This optimal ratio was established based on the result in Figure S8C. This mixture was heated to 90 °C and gradually cooled to room temperature over 2 hrs. In a typical assay, a reaction mixture containing target (T) of varying concentrations, 2 nM BDW/S/W triplex, 40 nM fuel (F), and 500 pM F-Track in 1 × CutSmart buffer was incubated at 37 °C for 3 hrs. The mixture was then transferred to the well of a 96 microplate and mixed with 10 U nicking endonuclease. Fluorescence signals were

measured immediately after adding the nicking enzyme using the same protocol outlined above.

Detection of Antibody. In a typical assay for the detection of antibody, a reaction mixture containing anti-biotin antibodies of varying concentrations and 10 nM biotinylated BDW was incubated at 37 °C for 30 min. This reaction mixture was then mixed with 500 pM F-Track and 10 U nicking endonuclease and measured using the same protocol as outlined above. The final concentration of BDW was 1 nM in the final solution.

ASSOCIATED CONTENT

Supporting Information. The Supporting Information is available free of charge *via* the Internet at http://pubs.acs.org. The supplementary table S1 provides details of sequence design. Figure S1-S12 provide detailed characterization of DNA walkers in terms of kinetics, spacer length, spacer rigidity, intraparticle walking, substrate density, and stability, and optimization of sequence design for nucleic acid and protein biosensors,

AUTHOR INFORMATION

Corresponding Author

*Feng Li, fli@brocku.ca

ACKNOWLEDGMENT

We thank the National Science and Engineering Research Council of Canada, the Ontario Ministry of Research, Innovation and Science, the China Scholarship Council, and the Brock University Start-Up Fund for financial supports.

REFERENCES

(1) Rosi, N. L.; Mirkin, C. A. Nanostructures in Biodiagnostics. *Chem. Rev.* **2005**, *105*, 1547-1562.

(2) Farka, Z.; Jurik, T.; Kovar, D.; Trnkova, L.; Skladal, P. Nanoparticle-Based Immunochemical Biosensors and Assays: Recent Advances and Challenges. *Chem. Rev.* **2017**, *117*, 9973-10042.

(3) Saha, K.; Agasti, S. S.; Kim, C.; Li, X.; Rotello, V. M. Gold Nanoparticles in Chemical and Biological Sensing. *Chem. Rev.* **2012**, *112*, 2739-2779.

(4) Rosi, N. L.; Giljohann, D. A.; Thaxton, C. S.; Lytton-Jean, A. K. R.; Han, M. S.; Mirkin, C. A. Oligonucleotide-Modified Gold Nanoparticles for Intracellular Gene Regulation. *Science,* **2006**, *312*, 1027–1031.

(5) Chen, G.; Roy, I.; Yang, C.; Prasad, P. N. Nanochemistry and Nanomedicine for Nanoparticle-Based Diagnostics and Therapy. *Chem. Rev.* **2016**, *116*, 2826-2885.

(6) Willner, I.; Willner, B. Biomolecule-Based Nanomaterials and Nanostructures. *Nano Lett.* **2010**, *10*, 3805–3815.

(7) Gao, J.; Gu, H.; Xu, B. Multifunctional Magnetic Nanoparticles : Design , Synthesis , and Biomedical Applications. *Acc. Chem. Res.* **2009**, *42*, 1097–1107.

(8) Erathodiyil, N.; Ying, J. Y. Functionalization of Inorganic Nanoparticles for Bioimaging Applications. *Acc. Chem. Res.* **2011**, *44*, 925–935.

(9) Algar, W. R.; Jeen, T.; Massey, M.; Peveler, W. J.; Asselin, J. Small Surface, Big Effects, and Big Challenges: toward Understanding Enzymatic Activity at the Inorganic Nanoparticle − Substrate Interface. *Langmuir,* **2019,** *35*, 7067-7091.

(10) Johnson, B. J.; Algar, W. R.; Malanoski, A. P.; Ancona, M. G.; Medintz, I. L. Understanding Enzymatic Acceleration at Nanoparticle Interfaces: Approaches and Challenges. *Nano Today* **2014**, *9*, 102−131.

(11) Hill, H. D.; Millstone, J. E.; Banholzer, M. J.; Mirkin, C. A. The Role Radius of Curvature Plays in Thiolated Oligonucleotide Loading on Gold Nanoparticles. *ACS Nano* **2009**, *3*, 418–424.

(12) Liu, L.; Xu, K.; Wang, H.; Tan, P. K.; Fan, W.; Venkatraman, S. S.; Li, L.; Yang, Y. Y. Self-Assembled Cationic Peptide Nanoparticles as an Efficient Antimicrobial Agent. *Nat. Nanotechnol.* **2009**, *4*, 457-463.

(13) Vranish, J. N.; Ancona, M. G.; Walper, S. A.; Medintz, I. L. Pursuing the Promise of Enzymatic Enhancement with Nanoparticle Assemblies. *Langmuir,* **2018**, *34*, 2901−2925

(14) Algar, W. R.; Malonoski, A.; Deschamps, R.; Blanco-canosa, J. B.; Susumu, K.; Stewart, M. H.; Johnson, B. J.; Dawson, P. E.; Medintz, I. L. Proteolytic Activity at Quantum Dot-Conjugates: Kinetic Analysis Reveals Enhanced Enzyme Activity and Localized Interfacial “Hopping”. *Nano Lett.* **2012**, *12*, 3793–3802.

(15) Seferos, D. S.; Prigodich, A. E.; Giljohann, D. A.; Patel, P. C.; Mirkin, C. A. Polyvalent DNA Nanoparticle Conjugates Stabilize Nucleic Acids. *Nano Lett.* **2009**, 308–311.

(16) Prigodich, A. E.; Alhasan, A. H.; Mirkin, C. A. Selective Enhancement of Nucleases by Polyvalent DNA-Functionalized Gold Nanoparticles. *J. Am. Chem. Soc.* **2011**, *133*, 2120–2123.

(17) Mason, S.; Tang, Y.; Li, Y.; Xie, X.; Li, F. Emerging Bioanalytial Applications of DNA Walkers. *Trends Anal. Chem.*, **2018**, *107*, 212-221.

(18) Zhang, H.; Lai, M.; Zuehlke, A.; Peng, H.; Li, X. F.; Le, X. C. Binding-Induced DNA Nanomachines Triggered by Proteins and Nucleic Acids. *Angew. Chem. Int. Ed.* **2015**, *54*, 14326–14330.

(19) Yang, X.; Tang, Y.; Mason, S. D.; Chen, J.; Li, F. Enzyme-Powered Three-Dimensional DNA Nanomachine for DNA Walking, Payload Release, and Biosensing. *ACS Nano* **2016**, *10*, 2324–2330.

(20) Qu, X.; Zhu, D.; Yao, G.; Su, S.; Chao, J.; Liu, H.; Zuo, X.; Wang, L.; Shi, J.; Wang, L.; Huang, W.; Pei, H.; Fan, C. An Exonuclease III-Powered, On-Particle Stochastic DNA Walker. *Angew. Chem. Int. Ed.* **2017**, *56*, 1855-1858.

(21) Li, Y.; Wang, G, A.; Mason, S. D.; Yang, X.; Yu, Z.; Tang, Y.; Li, F. Simulation-Guided Engineering of an Enzyme-Powered Three Dimensional DNA Nanomachine for Discriminating Single Nucleotide Variants. *Chem. Sci.* **2018**, *9*, 6434-6439.

(22) Li, F.; Zhang, H.; Dever, B.; Li, X.-F.; Le, X. C. Thermal Stability of DNA Functionalized Gold Nanoparticles. *Bioconjugate Chem*. **2013**, 24, 1790−1797.

(23) Hurst, S. J.; Lytton-Jean, A. K.; Mirkin, C. A. Maximizing DNA Loading on a Range of Gold Nanoparticle Sizes. *Anal. Chem.* **2006**, 78, 8313−8318.

(24) Zhang, D. Y.; Turberfield, A. J.; Yurke, B.; Winfree, E. Engineering Entropy-Driven Reactions and Networks Catalyzed by DNA. *Science* **2007**, *318*, 1121-1125.

(25) Porchetta, A.; Ippodrino, R.; Marini, B.; Caruso, A.; Caccuri, F.; Ricci, F. Programmable Nucleic Acid Nanoswitches for the Rapid, Single-Step Detection of Antibodies in Bodily Fluids. *J. Am. Chem. Soc.* **2018**, *140*, 947-953.

(26) Ranallo, S.; Prevost-Tremblay, C.; Idili, A.; Vallee-Belisle, A.; Ricci, F. Antibody-Powered Nucleic Acid Release Using a DNA-Based Nanomachine. *Nat. Commun.* **2017**, *8*, 15150.

(27) Ranallo, S.; Rossetti, M.; Plaxco, K. W.; Vallee-Belisle, A.; Ricci, F. A Modular, DNA-Based Beacon for Single-Step Fluorescence Detection of Antibodies and Other Proteins. *Angew. Chem. Int. Ed.* **2015**, *54*, 13214-13218.

(28) Mahshid, S. S.; Camire, S.; Ricci, F.; Vallee-Belisle, A. A Highly Selective Electrochemical DNA-based Sensor that Employs Steric Hindrance Effects to Detect Protein Directly in Whole Blood. *J. Am. Chem. Soc.* **2015**, *137*, 15596-15599.

(29) Jung, C.; Allen, P. B.; Ellington, A. D. A Stochastic DNA Walker that Traverses a Microparticle Surface. *Nat. Nanotechnol.* **2016**, *11*, 157-163.

(30) Demers, L. M.; Mirkin, C. A.; Mucic, R. C.; Reynolds, R. A.; Letsinger, R. L.; Elghanian, R.; Viswanadham, G. A Fluorescence-Based Method for Determining the Surface Coverage and Hybridization Efficiency of Thiol-Capped Oligonucleotides Bound to Gold Thin Films and Nanoparticles. *Anal. Chem*. **2000**, 72, 5535−5541.

TOC